Molecular Therapy
Nucleic Acids
Original Article

CRISPR-based VEGF suppression using paired guide RNAs for treatment of choroidal neovascularization

Sook Hyun Chung,[1] Tzu-Ni Sin,[1] Brian Dang,[1] Taylor Ngo,[1] Therlinder Lo,[1] Daniella Lent-Schochet,[1] Ratheesh K. Meleppat,[1] Robert J. Zawadzki,[1] and Glenn Yiu[1]

[1]Department of Ophthalmology and Vision Science, UC Davis Health, UC Davis Eye Center, University of California, Davis, Davis, CA 95616, USA

Clustered regularly interspaced short palindromic repeats (CRISPR)-based genomic disruption of vascular endothelial growth factor A (*Vegfa*) with a single gRNA suppresses choroidal neovascularization (CNV) in preclinical studies, offering the prospect of long-term anti-angiogenesis therapy for neovascular age-related macular degeneration (AMD). Genome editing using CRISPR-CRISPR-associated endonucleases (Cas9) with multiple guide RNAs (gRNAs) can enhance gene-ablation efficacy by augmenting insertion-deletion (indel) mutations with gene truncations but may also increase the risk of off-target effects. In this study, we compare the effectiveness of adeno-associated virus (AAV)-mediated CRISPR-Cas9 systems using single versus paired gRNAs to target two different loci in the *Vegfa* gene that are conserved in human, rhesus macaque, and mouse. Paired gRNAs increased *Vegfa* gene-ablation rates in human cells *in vitro* but did not enhance VEGF suppression in mouse eyes *in vivo*. Genome editing using paired gRNAs also showed a similar degree of CNV suppression compared with single-gRNA systems. Unbiased genome-wide analysis using genome-wide unbiased identification of double-stranded breaks (DSBs) enabled by sequencing (GUIDE-seq) revealed weak off-target activity arising from the second gRNA. These findings suggest that *in vivo* CRISPR-Cas9 genome editing using two gRNAs may increase gene ablation but also the potential risk of off-target mutations, while the functional benefit of targeting an additional locus in the *Vegfa* gene as treatment for neovascular retinal conditions is unclear.

INTRODUCTION

Pathologic ocular angiogenesis in retinopathy of prematurity, proliferative diabetic retinopathy, and neovascular age-related macular degeneration (nAMD) are leading causes of vision loss among individuals across their lifetime.[1] Aberrant proliferation of retinal or choroidal vessels in these conditions results in fluid exudation, hemorrhage, and even retinal detachment that can compromise visual function. Among various regulators of pathologic angiogenesis, the most established pro-angiogenic factors in the eye belong to the vascular endothelial growth factor (VEGF) family, among which VEGFA is considered the most potent.[2–4] VEGFA expression is upregulated in eyes with nAMD, and most current therapies involve intraocular delivery of humanized antibodies (bevacizumab), antibody fragments (ranibizumab, brolucizumab), and decoy receptor proteins (aflibercept) that are directed against secreted isoforms of VEGF.[5,6] Despite their positive impact on patients' vision, frequent intraocular injections of these biologic agents are invasive, carry a risk of endophthalmitis, and pose a heavy clinical and financial burden for patients and the healthcare system. Among approaches to improve the durability of these treatments, viral-based gene therapy may enable long-term production of anti-angiogenesis agents *in vivo*, with several clinical trials underway (ClinicalTrials.gov: NCT04645212, NCT04704921, NCT04514653, NCT04567550).[7–9]

Clustered regularly interspaced short palindromic repeats (CRISPR)-based strategies have the potential to permanently suppress pro-angiogenic factors at the genome level. By employing programmable guide RNAs (gRNAs) to direct prokaryotic CRISPR-associated endonucleases (Cas9) to induce site-specific insertion-deletion (indel) and frameshift mutations to ablate the target gene,[10] CRISPR-based anti-angiogenesis therapies could provide a permanent cure rather than the repeated treatments that are currently in use. Genomic ablation of *VEGFA* using Cas9 has been demonstrated in human retinal pigment epithelial (RPE) cells *in vitro*[11] and in mouse eyes using ribonucleoprotein, adeno-associated virus (AAV),[12–14] or lentiviral vector delivery *in vivo*.[15,16] CRISPR systems have also been used to disrupt upstream and downstream pro-angiogenic signals such as hypoxia inducible factor 1α (Hif-1α)[14] and VEGF receptor 2 (VEGFR-2).[13] Comparisons of different Cas9 orthologs suggest that some variants such as *S. pyogenes* Cas9 (SpCas9) may be more effective than *S. aureus* Cas9 (SaCas9) in suppressing VEGFA protein levels, despite the larger gene size of SpCas9 requiring the use of two separate AAV vectors for delivery.[12] However, the potential benefit or risk of using additional gRNAs for clinical translation remains unclear.

Received 3 November 2021; accepted 23 April 2022;
https://doi.org/10.1016/j.omtn.2022.04.015.

Correspondence: Glenn Yiu, Department of Ophthalmology & Vision Science, University of California, Davis, 4860 Y St., Suite 2400, Sacramento, CA 95817, USA.
E-mail: gyiu@ucdavis.edu

The use of multiple gRNAs in CRISPR-Cas9 gene editing can improve genomic disruption by enabling gene truncations and inversions in addition to indel mutations.[17] The first human trial using CRISPR-Cas9 gene editing in the eye employs paired gRNAs to remove the aberrant splice donor in the CEP290 gene mutation in patients with type 10 Leber congenital amaurosis.[18] However, the additional gRNAs may also increase the risk of off-target activity by increasing the number of non-specific gene loci that may be inadvertently mutated. Most current studies assess putative off-target sites using *in silico* predictions that assume that off-target sites are closely related to on-target sequences but may underestimate non-specific adverse effects of CRISPR-based genome editing.

In this study, we compare the efficacy and safety of single versus paired gRNAs in an AAV-mediated CRISPR-Cas9 platform to suppress VEGFA in a mouse model of laser-induced choroidal neovascularization (CNV). We selected gRNAs to target regions of the *Vegfa* gene that are conserved between mice, rhesus macaques, and humans to enable preclinical testing in non-human primates and future translation to AMD patients. We hypothesize that paired gRNAs will improve the efficiency of *Vegfa* gene disruption and CNV suppression. Importantly, we also compare potential off-target activity between single and paired gRNAs in our platform using unbiased, genome-wide methodologies.

RESULTS

CRISPR-Cas9 disruption of human *VEGFA* gene using paired gRNAs *in vitro*

VEGFA has a well-established role in pathologic angiogenesis in the eye and is the principle therapeutic target for current treatments of retinal neovascular conditions. Since *VEGFA* is alternatively spliced to produce multiple isoforms, we targeted exon 1, which is common to all major isoforms and encodes the receptor-binding domain that is critical for VEGFA signaling, homodimerization, and receptor binding.[19] We explored the ~600 bp protein-coding region of exon 1 of the *Vegfa* gene in mouse, rhesus macaque, and human genomes to identify 8 gRNA target sites that are conserved across all three species and ranked them based on their predicted on- and off-target probabilities *in silico* (Figure 1A). Due to the limited packaging capacity of AAVs, we deployed SpCas9 and gRNA in two separate constructs, including an AAV vector to express SpCas9 under a cytomegalovirus (CMV) promoter (px551-CMV-SpCas9) and another to express one or two gRNAs under independent U6 promoters (px552), as well as green fluorescent protein (GFP) under a CMV promoter (Figure 1B). We first transfected human embryonic kidney 293T (HEK293T) cells with AAV-vector plasmids expressing SpCas9 and each of the 8 single gRNAs in a 1:1 molar ratio and found that gRNA1 and gRNA2 (Figure 1C), which had the highest predicted on- and off-target scores *in silico*, demonstrated the highest degree of indel mutations based on deep sequencing (Figure 1D). Unlike CRISPR-Cas9 platforms that utilize a single gRNA that can only generate indel mutations, possible outcomes of genome editing using paired gRNAs include (1) no editing, (2) indel mutations at either or both loci resulting in mostly frameshift mutations, and (3) truncation or inversion of the region between the gRNA targets (Figure 1E). We then transfected HEK293T cells with the AAV-vector plasmids expressing SpCas9 and either single (gRNA1 only), paired (gRNA1 + gRNA2), or empty (neither) gRNA and confirmed that genome editing using paired gRNA enables gene truncation by polymerase chain reaction (PCR) (Figure 1F). Deep sequencing demonstrated an 87.5% mutation of *Vegfa* consisting of truncations (82.3%), inversions (3.9%), and indel mutations (0.52%) using paired gRNAs, while a single gRNA produced only a 52.9% indel mutation (Figure 1G). Enzyme-linked immunosorbent assay (ELISA) demonstrated 25% ± 3.4% ($p = 0.02$) suppression of VEGFA protein using paired gRNAs compared with 17% ± 4.1% ($p = 0.09$) reduction using from a single-gRNA system (Figure 1H). These data suggest that *Vegfa* gene editing is more efficient using paired gRNAs than single gRNAs *in vitro* but that it does not translate linearly to VEGFA protein suppression in this setting.

CRISPR-Cas9 disruption of mouse *Vegfa* gene using paired gRNAs *in vivo*

For *in vivo* studies, we packaged the constructs into AAV serotype 8 (AAV8) vectors, which effectively transduces most outer retinal cell types in mouse eyes including RPE after subretinal injections.[16,17] We subretinally injected AAV8 vectors expressing SpCas9 and gRNAs in 1:1 ratio (5×10^{11} vg/eye) then performed fundus imaging to confirm adequate transduction efficiency (Figure S1). We then isolated RPE cells for deep sequencing to measure gene ablation and ELISA to measure VEGFA protein expression after 3 weeks (Figure 2A). Deep sequencing showed 33% gene disruption of *Vegfa* using paired gRNAs *in vivo*, with 16% truncation, 17% indel (97% frameshift, 3% in frame) mutations, and no detectable inversions, while single gRNAs produced 28% indel (90% frameshift, 10% in frame) mutations (Figure 2B). The CRISPR system using paired gRNAs suppressed VEGFA protein production by 37% ± 5.2% ($p = 0.001$) compared with empty gRNA, whereas single-gRNA CRISPR resulted in 24% ± 7.2% ($p = 0.03$) of suppression, with no significant difference between single- or paired-gRNA systems ($p = 0.16$) *in vivo* (Figure 2C).

CRISPR-mediated CNV suppression using paired gRNAs *in vivo*

For functional validation, we performed laser-induced CNV at 3 weeks after subretinal AAV injections and evaluated CNV size by measuring lesion area as seen on fluorescence angiography (FA), optical coherent tomography angiography (OCT-A), and flatmount immunohistochemistry with an endothelial cell marker at 1 week after laser injury. Compared with eyes that received dual AAV8 vectors expressing SpCas9 and empty gRNA control, those that had AAV8 expressing SpCas9 with single or paired gRNAs demonstrated a 19%–20% reduction in CNV area as measured on OCT-A, with no significant difference between these two groups (Figures 3A and 3B). Likewise, immunohistochemistry using isolectin B4 showed that CRISPR-Cas9 suppression of VEGFA using either single or paired gRNAs resulted in approximately 30% smaller CNV lesion size compared with empty gRNA controls (Figures 3C and 3D). Thus, our findings suggest that despite greater VEGF suppression

A

gRNA Name	Target Sequence (5'-3')	Mouse PAM	Mouse On Target Score	Mouse Off Target Score	Rhesus Macaque PAM	Rhesus Macaque On Target Score	Rhesus Macaque Off Target Score	Human PAM	Human On Target Score	Human Off Target Score
gRNA1	CAGAAAGTTCATGGTTTCGG	AGG	60.55	43.55	AGG	60.55	43.55	AGG	60.55	43.55
gRNA2	GAGAAGTGCTAGCTCGGGCC	TGG	49.55	45.54	GGG	54.04	45.54	GGG	54.04	45.54
gRNA3	AGAGGGAGCGCGAGCCGCGC	CGG	47.32	44.05	CGG	47.32	44.05	CGG	46.30	44.05
gRNA4	CTCGCGCTCCCTCTCCGGCT	CGG	46.62	44.82	GGG	37.44	39.53	GGG	37.44	39.53
gRNA5	AAACTTTTCGTCCAACTTCT	GGG	37.08	39.53	CGG	36.43	44.82	CGG	36.43	44.82
gRNA6	CGCGGCTCGCGCTCCCTCTC	CGG	34.57	43.20	CGG	35.58	43.20	CGG	34.57	43.20
gRNA7	AGCGCGAGCCGCGCCGGCCC	CGG	32.69	45.34	CGG	34.42	45.34	CGG	33.40	45.34
gRNA8	GAAACTTTTCGTCCAACTTC	TGG	26.44	41.49	TGG	26.80	41.49	TGG	26.80	41.49

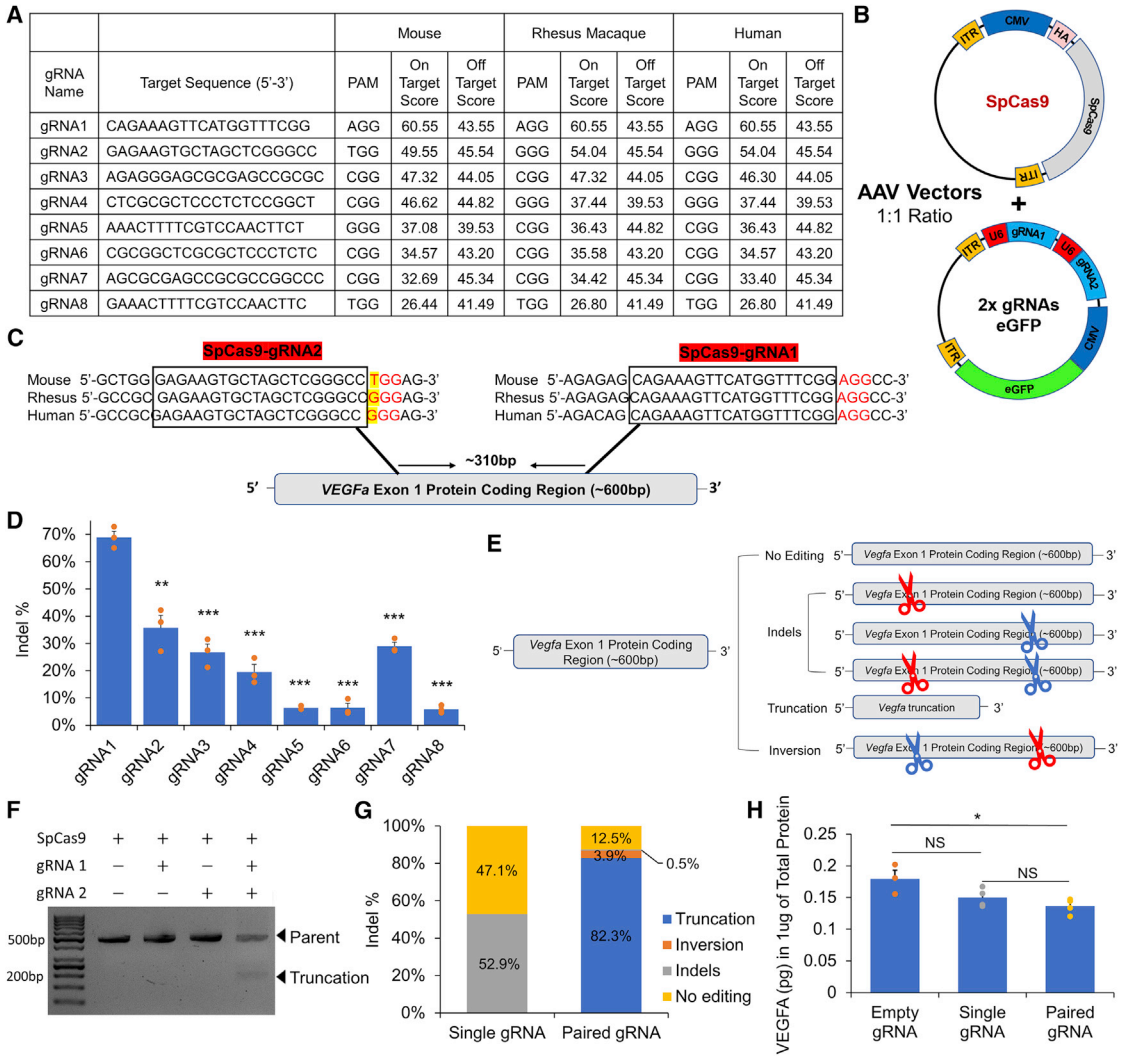

Figure 1. Design and efficacy of a CRISPR system using paired gRNA to suppress VEGF in human cells *in vitro*

(A) Table listing all gRNA target sequences conserved across mouse, rhesus macaque, and humans with predicted on-target gene-editing efficiency and off-target probability scores. (B) Schematic of AAV vectors to express hemagglutinin (HA)-tagged SpCas9 under a CMV promoter and paired gRNAs under independent U6 promotors with a CMV-promoter-driven EGFP reporter. (C) Comparison of the two gRNAs (gRNA1 and gRNA2) with the highest predicted on-target scores targeting two loci, located 310 bp apart, in the exon 1 protein-coding region of the *VEGFA* gene that are conserved across the three species. (D) Bar graph comparing indel frequency of gRNA1 with the other 7 gRNAs based on deep sequencing of PCR amplicons of *VEGFA* gene from HEK293T cells transfected with plasmids shown in (B) (n = 3). (E) Outline of possible genome-editing scenarios using a paired-gRNA system. (F and G) Gel electrophoresis (F) and deep sequencing (G) of PCR amplicons of *VEGFA* gene from HEK293T cells transfected with plasmids shown in (B), demonstrating gene truncation using paired gRNAs (n = 3). (H) Bar graphs comparing VEGF protein levels measured from ELISA 48 h post transfection (n = 5). NS, not significant. *$p < 0.05$, **$p < 0.01$, and ***$p < 0.001$ (Student's t test). Error bar represents SEM.

using paired versus single gRNAs in human cells *in vitro*, viral-mediated delivery of this CRISPR-Cas9 system to mouse eyes *in vivo* did not show a functional benefit using additional gRNAs.

Off-target effects from CRISPR-Cas9 using paired gRNAs

To measure off-target editing activity in human cells, we transfected HEK293T cells with the AAV vector plasmids expressing SpCas9 and either single (gRNA1 or gRNA2) or paired (gRNA1 + gRNA2) gRNAs in a 1:1 ratio and performed genome-wide unbiased identification of double-stranded breaks (DSBs) enabled by sequencing (GUIDE-seq) analysis, which can detect off-target activities as low as 0.1%.[20] We identified no significant off-target activity in the gRNA1-only group (Figure 4A), a weak off-target site (3.6% detected) located in the intron of Rap guanine nucleotide exchange factor 2 (RAPGEF2) on chromosome 4 from the gRNA2-only group (Figure 4B), and a very minor off-target (0.6% detected) site in the intron of the microtubule-associated monooxygenase, calponin and LIM domains-containing 3 (MICAL3) gene on chromosome 22 from the

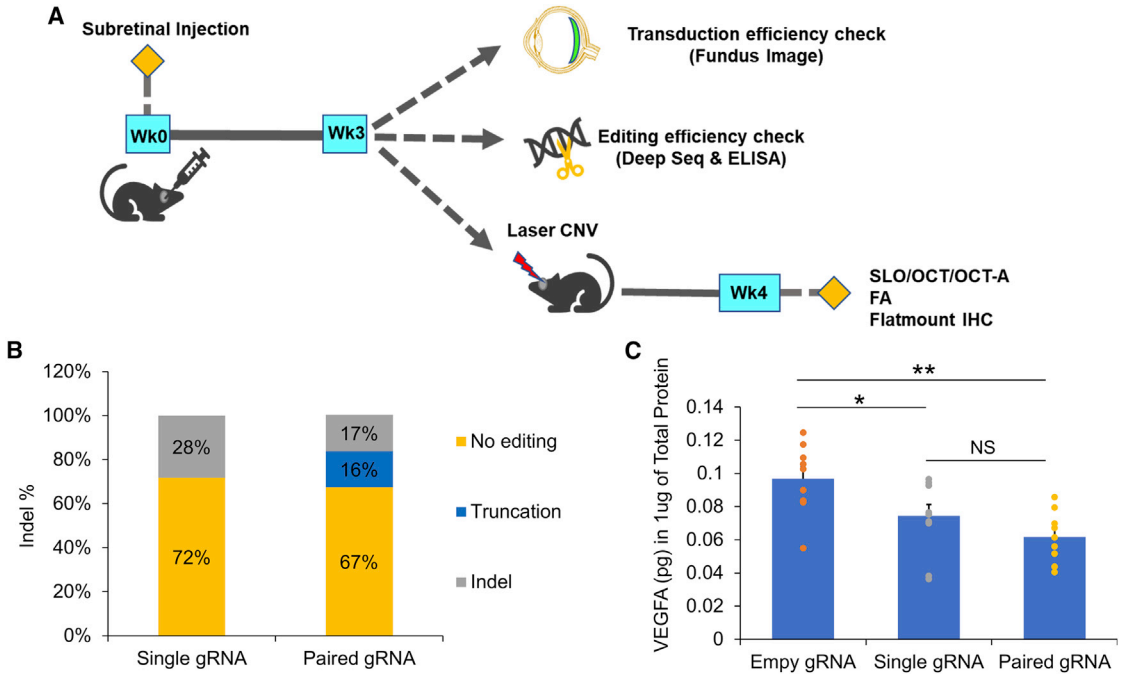

Figure 2. Efficacy of a CRISPR system using paired gRNAs to suppress VEGF in mouse eyes *in vivo*

(A) Schematic of study design using subretinal AAV8 to deliver SpCas9 with paired gRNAs to suppress VEGF, followed by confirmation of transduction efficiency by fundus imaging and measurement of gene-editing rates and protein suppression by deep sequencing and ELISA, respectively, after 3 weeks, as well as suppression of laser-induced CNV after 4 weeks. (B and C) Bar plots comparing gene-editing rates from deep sequencing of PCR amplicons of *Vegfa* from mouse RPE cells (B) (n = 7–9), and VEGF protein levels measured from ELISA (C) (n = 10). NS, not significant. *p < 0.05 and **p < 0.01 (Student's t test). Error bar represents SEM.

paired-gRNA group (Figure 4C). Although these weak off-target mutations were detected at very low levels, both appear to arise from gRNA2 activities.

DISCUSSION

Anti-VEGF pharmacotherapies have revolutionized the management of neovascular retinal diseases, but frequent intraocular injections remain a clinical burden for patients and physicians. Several ongoing clinical trials are currently exploring the use of viral vectors to provide long-term intraocular expression of soluble anti-angiogenesis agents. Unlike these gene-therapy approaches, CRISPR-based genome editing enables permanent ablation of pro-angiogenic factors, targeting of both intracellular and extracellular signals, and potential for cell-specific delivery that can target more pathologically relevant cellular sources. Viral vector-mediated CRISPR-Cas9 has been used to suppress VEGF as well as upstream and downstream signals such as Hif-1α and VEGFR-2.[15,21,22] However, the optimal system remains unclear due to heterogeneity in experimental methodology, differences in functional readouts, and relative lack of comparative studies. Our group previously compared an "all-in-one" AAV vector that combines the smaller SaCas9 ortholog and gRNAs with a dual-AAV system that expresses SpCas9 and gRNAs on separate vectors. We found that the latter approach demonstrated greater levels of genome editing and protein suppression, with up to 35% VEGF reduction in mouse eyes *in vivo*. Here, we examined whether the addition of a second gRNA targeting *Vegfa* to this genome-editing platform could enhance anti-angiogenesis activity and, importantly, if safety would be compromised by a concomitant increase in risk of harmful mutations.

Our study found that CRISPR-Cas9 with paired gRNAs increased *Vegfa* gene ablation with a slight increase in off-target activity in human cells *in vitro* but that it did not appear to improve VEGF or CNV suppression in mouse eyes *in vivo*. The discordance between *in vitro* and *in vivo* findings is not surprising, as the latter may be impacted by many additional biological variables including (1) interspecies differences, (2) viral transduction efficiency, (3) homeostatic responses, and (4) limitations of the laser-induced CNV model. We designed gRNAs to target conserved sequences of the *Vegfa* gene across mice, rhesus macaques, and humans to enable clinical translation, and *in silico* predictions of on-target and off-target activities were similar across all three species. However, *in vivo* studies may also be impacted by variability in viral transduction efficiency, surgical artifacts from the subretinal injection procedure, or method of RPE cell isolation. The single- and paired-gRNA-expressing vectors are similar in size (5.5 versus 5.9 kB) and appeared to exhibit consistent widespread AAV transduction based on GFP reporter expression after subretinal injection (Figure S1), consistent with measurements of viral genome per diploid mouse genomes, as we have previously shown.[12] We also excluded eyes with surgical complications such as

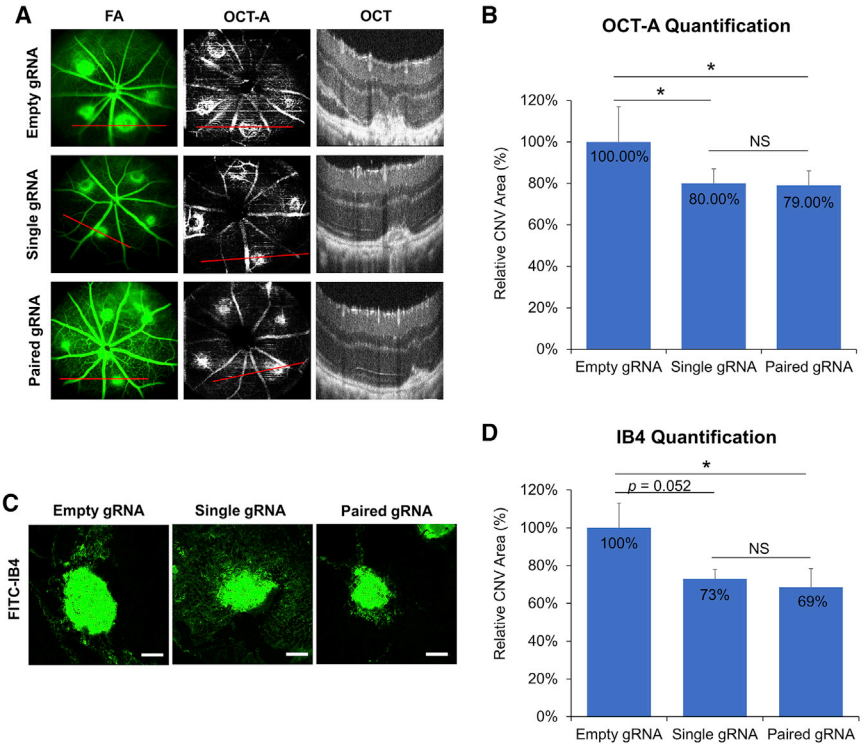

Figure 3. A CRISPR system using paired gRNAs to target *Vegfa* suppressed laser-induced choroidal neovascularization in mouse eyes

(A–D) Multimodal imaging using fluorescein angiography (FA), optical coherence tomography (OCT), and OCT angiography (OCT-A) (A), and bar plots comparing CNV area measured from *in vivo* imaging (n = 20–33) (B), as well as representative fluorescence images of flat mount immunohistochemistry using isolectin B4 (scale bars, 100 μm) (C) and bar plots comparing CNV area measured from these *ex vivo* images (n = 26–30) from mouse eyes after AAV-mediated delivery of SpCas9 with paired gRNAs targeting *Vegfa* (D). NS, not significant. *$p < 0.05$ (Student's t test). Error bar represents SEM.

hemorrhage, infection, or cataract formation and only included eyes with broad expression as seen on *in vivo* imaging. In the outer retina, VEGF is primarily produced by RPEs, but glial and immune cells including macrophages, activated T cells, and leukocytes can also secrete VEGF.[23–26] Although we isolated RPE cells to enrich for VEGF-expressing cells, homeostatic responses from non-transduced or non-edited cells, or other compensatory pro-angiogenic pathways, may account for the lack of performance difference between single and paired gRNAs. Future studies using single-cell transcriptomic analyses could identify the specific cell types that are successfully edited and how VEGF expression is differentially affected in various cell types. Also, although other VEGF family members such as VEGFB, VEGFC, and VEGFD are not considered to play as important a role as VEGFA in pathologic angiogenesis in the eye, additional studies to target multiple pro-angiogenic targets may be considered in the future.

In our experiments, we found that the degree of gene ablation did not translate linearly to protein suppression and that VEGF levels did not scale directly with CNV reduction. In fact, CNV suppression in our model did not exceed 31% using either single- or paired-gRNA systems, similar to prior studies where even therapeutic intravitreal doses of the clinically proven VEGF-inhibitor aflibercept only suppressed laser-induced CNV by about 40%, indicating a ceiling treatment effect in this disease model.[12,27] Although widely used for testing of anti-angiogenesis agents, the laser-induced CNV rodent model more likely reflects an injury response rather than chronic degeneration seen in AMD.[28] Thus, the potential therapeutic benefit of using CRISPR-based platforms for neovascular retinal diseases remains unclear. Nevertheless, as CRISPR systems have the potential advantage of simultaneously targeting several different pro-angiogenic factors by multiplexing gRNAs, additional research exploring combinatorial genome-editing approaches may be warranted.

The potential for permanent VEGF suppression using CRISPR-Cas9 is appealing but raises a concern for safety. Although VEGF promotes pathologic angiogenesis,[29] it also participates in normal vessel growth[30] and trophic maintenance of photoreceptors.[31] Thus, therapeutic benefit may only be maximized by striking a balance between pathologic and physiologic VEGF levels and targeting more pathologic cellular sources. For example, targeted delivery of short hairpin RNA (shRNA) to Müller glia to reduce VEGFA to more physiologic levels rescues oxygen-induced retinopathy (OIR) in rats without interfering with retinal vascular development,[32] while RPE-specific deletion of *Vegfa* causes choriocapillaris loss and photoreceptor dysfunction.[33] In fact, chronic anti-VEGF injections have been linked to geographic atrophy progression in AMD patients.[34,35] Thus, unlike current therapies that broadly suppress VEGF and may adversely impact non-pathologic vascular or neural tissues, viral-mediated CRISPR-Cas9 platforms may confer greater cell specificity to target more pathologic sources of angiogenic factors. The stochastic nature of CRISPR-based gene disruption also results in incomplete VEGF suppression, reducing the likelihood of harmful over-suppression.

Despite these potential advantages, the risk of deleterious off-target mutations with long-term Cas9 expression introduces another safety concern. In our study, the addition of a second gRNA appeared to generate a small but detectable amount of off-target activity in human cells, despite enhancing CRISPR-mediated ablation of the *Vegfa* gene. Unlike many studies that assess predicted off-target sites based on their resemblance to on-target sequences, we employed an unbiased genome-wide GUIDE-seq assay that has a sensitivity threshold of 0.1%. Although intravitreal delivery of AAV-CjCas9 targeting *Vegfa*

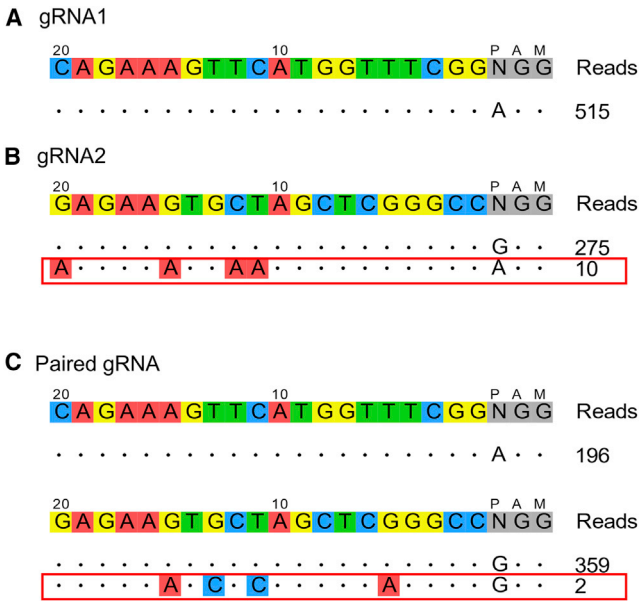

Figure 4. Comparison of off-target mutations between CRISPR systems using single and paired gRNAs to target *VEGFA*

(A–C) Results of GUIDE-seq analysis showing potential off-target rates using single (A and B) or paired gRNAs (C). HEK293T cells were transfected with plasmids to express SpCas9 and either single (gRNA1 or gRNA2) or paired (gRNA1 and gRNA2) gRNA, with MiSeq performed reading both + and - strands from double-stranded oligodeoxynucleotides (dsODN) representing CRISPR-editing sites. One weak off-target site (10 reads) was identified from gRNA2 (B, red box), and a minor off-target site (2 reads) was identified from paired gRNA1 + gRNA2 analyses (C, red box).

and *Hif-1α* in mouse retina also did not demonstrate any off-target activity after 14 months,[36] continued Cas9 expression over years could still pose a cumulative risk of harmful mutations. Additionally, genome editing can occasionally cause chromosomal translocations with reported rates exceeding 1%, as detected by methods such as linear amplification-mediated high-throughput genome-wide sequencing (LAM-HTGTS) or unidirectional targeted sequencing (UDiTaS).[37–40] While *in vivo* studies of genome editing for Duchenne muscular dystrophy using an AAV8 vector did not show any translocation using transposon-mediated target enrichment and sequencing, which has an estimated limit of detection of 0.01%,[41] future studies are needed to elucidate the risk of chromosomal translocations and other potentially harmful genetic events. Some strategies to reduce the duration of Cas9 exposure include ribonucleoprotein (RNP) delivery using lentiviral or lipid nanoparticles, optogenetic "on-off" switching of Cas9, and a self-targeting kamikaze CRISPR system.[16,42–47] Use of truncated gRNAs or engineered high-fidelity Cas9 orthologs also show promise in reducing off-target risks.

Finally, the host immune consequences of expressing a prokaryotic protein in the eye remain unknown. Although the subretinal space is an immune-privileged compartment, AAV-mediated expression of other foreign genes such as GFP triggers intraocular inflammation that may be associated with the amount of viral-vector egress from the eye.[48] Longer-term studies in larger preclinical animal models such as non-human primates will provide important data on long-term safety and host immune responses with sustained CRISPR-Cas9 expression.

MATERIALS AND METHODS

gRNA design and AAV constructs

gRNA design was performed *in silico* using Benchling software (San Francisco, CA, USA), which identified 8 gRNA target sites in exon 1 of *Vegfa* that are conserved across mouse, rhesus macaque, and human. gRNAs were cloned into a modified px552 plasmid (Addgene, Watertown, MA, USA, 60958), where we replaced the human synapsin (hSyn) promotor with a ubiquitous CMV promotor to drive GFP expression. We selected the two gRNAs (gRNA1 and gRNA2) with the highest on-target score that predicts gene-cleavage efficiency and the lowest off-target probability *in silico*, which corresponded to the highest indel frequency *in vivo*. We subcloned gRNA1 or gRNA2 upstream of the U6-driven gRNA scaffold using the SapI restriction site (px552-CMV-gRNA1 or px552-CMV-gRNA2). The DNA region containing the U6 promotor, gRNA1, and gRNA scaffold were amplified by PCR with PspOMI overhangs and subcloned into the px552-CMV-gRNA2 plasmid to generate a construct containing both gRNA1 and gRNA2 under two independent U6 promotors (px552-CMV-gRNA1/2). For the AAV vector expressing SpCas9, we modified the px551 plasmid (Addgene, 60957) by replacing the truncated methyl-CpG-binding protein 2 (pMecp2) promoter with a CMV promoter for *in vitro* studies and, later, with px551-CMV-SpCas9 (Addgene 107024) for *in vivo* studies.

Cell culture and transfection

HEK293T cells were maintained in Dulbecco's modified Eagle's medium (DMEM) containing 10% fetal calf serum and 1% penicillin and streptomycin. Cells were seeded in 24-well plates (1×10^5 cells/well) and transfected with 500 ng/well DNA using lipofectamine (Invitrogen, Waltham, MA, USA, 116680027) according to the manufacturer's protocol. Cells were collected for genomic DNA extraction 48 h after transfection using Qiagen DNeasy Blood and Tissue kit (Qiagen, Germantown, MD, USA, 69504).

Deep sequencing

After genomic DNA extraction, a NanoDrop 2000c device (Thermo Fisher Scientific, Waltham, MA, USA) was used to verify the quality and quantity of the DNA then was amplified through PCR using forward and reverse primers for 35 cycles of 98°C for 10 s, 60°C for 30 s, and 72°C for 15 s. The primer sets included 5′-GCGGCGTCGCACTGAAACTTT-3′ (forward) and 5′-AGCAGGGCACGACCGCTTA-3′ (reverse) for HEK293T cells (primers are approximately 100 bp from the gRNA sites, and the total amplicon size is 500 bp) and 5′-TTCGTCCAACTTCTGGGCTCTTCTC-3′ (forward) and 5′-CACGACCGCTTACCTTGGCA- 3′ (reverse) for mouse RPE tissues (primers are approximately 100 bp from the gRNA sites, and the total PCR amplicon size is 450 bp). The PCR products were purified with the QIAquick PCR purification kit (Qiagen, 28104), and deep sequencing was conducted at the DNA sequencing core facility at Massachusetts General Hospital (Boston, MA, USA).

AAV-virus production

AAV constructs were packaged into AAV8 capsids and purified by the UC Davis Center for Vision Sciences Molecular Construct and Packaging core facility. Viral titers were determined by Taqman quantitative PCR ,and purity was assessed by SDS-polyacrylamide gel electrophoresis.

Animals and subretinal injections

All animal experiments were conducted under the guidelines of the Institutional Animal Care and Use Committee (IACUC) at UC Davis. C57BL/6J mice (Jackson Laboratory, Bar Harbor, ME, USA) were kept in standard 12 h light/dark cycle. For subretinal injections, animals were anesthetized with 2% isoflurane, and eyes were dilated with 1% tropicamide and 2.5% phenylephrine. After creating a small conjunctival peritomy and a paralimbal sclerotomy using a 30G needle, 2 uL of the AAV8-vector mixture was injected using a 31G Hamilton syringe into the subretinal space (5×10^{11} vg/eye), with AAVs expressing SpCas9 and gRNA mixed at a 1:1 ratio prior to injection.

RPE isolation

RPEs were isolated using an established protocol with minor modification.[49] Briefly, after enucleation, the anterior chamber, lens, and retina were removed, and the posterior eye cup was incubated with 0.05% trypsin-EDTA for 45 min at 37°C. After gentle shaking of the eye cup to isolate the RPEs, cell pellets were collected for genomic DNA extraction using DNeasy Blood & Tissue kit (Qiagen, 69504). For protein extraction, posterior eye cups containing RPE and choroidal tissues were mechanically homogenized with radioimmunoprecipitation assay (RIPA) buffer, and protein quantification performed using a Pierce BCA protein assay kit (Thermo Fisher Scientific, 23225).

ELISA

We used a human VEGF ELISA kit (Invitrogen, KHG0111) for HEK293T cell extracts, and a mouse VEGF ELISA kit (R&D Systems, Minneapolis, MN, USA, MMV00) for mouse RPE protein samples, following the manufacturer's protocol. In short, samples were prepared in a 1:50 dilution and incubated on a precoated plate for 2 h, followed by conjugate and substrate solutions. The optical density was measured using a microplate reader at 450 nm, and VEGFA quantification was calculated against the linear portion of the standard curve. Each sample was run in triplicates.

Laser-induced CNV and fluorescein angiography

Animals were anesthetized with isoflurane inhalation, and pupils were dilated with 1% tropicamide and 5% phenylephrine. Mice were imaged using the Micron IV system (Phoenix, Pleasanton, CA, USA) with topical artificial tear gel (Genteal) to prevent corneal damage. Image-guided laser photocoagulation was performed with a 532 nm wavelength laser at 250 mW for 70 ms. CNV was evaluated by FA, OCT, and OCT-A 1 week after laser photocoagulation. Eyes with severe hemorrhage were excluded from analyses.

OCT and OCT-A imaging

OCT and OCT-A imaging were performed using a custom multimodal OCT + scanning laser ophthalmoscopy (SLO) imaging system at the UC Davis small animal ocular imaging facility (EyePod), as previously reported.[50] SLO and phase-variance OCT-A images were acquired simultaneously with a SLO excitation laser (ORBIS 488LX, Coherent, Salem, NH, USA) running at 488 nm with 100 μW at the mouse pupil and OCT with a superluminescent diode light source (Broadlighter 860, Superlum Diodes, Cork, Ireland) operating at 860 nm with full width at half maximum (FWHM) of 132 nm and 600 uW at the mouse pupil, respectively. For SLO, reflected and fluorescent light was captured by two photomultiplier tubes (H7422–20 and H7422-40, Hamamatsu Photonics, Shizuoka, Japan), and 50 consecutive images were averaged. For OCT-A, 1080 horizontal B scans acquired with a series of three scans per single location (spanning 540 × 360 pixels) corresponding to the SLO images were captured with a custom spectrometer with a high-speed line complementary metal-oxide semiconductor (CMOS) camera (Sprint spL4096-140km, Basler, Ahrensburg, Germany) and used for 3-dimestional cross-sectional visualization and co-registration.

OCT segmentation, OCT-A imaging, and CNV quantification

A custom, semi-automated CNV segmentation program written in MATLAB (MathWorks, Natick, MA, USA) was used to segment and visualize the CNV between the external limiting membrane (ELM) and RPE layer from the OCT images. Briefly, 10–15 B scans were selected from the OCT volume, then 10–15 pixel points were manually annotated along the OPL and RPE layers, allowing interpolation (spline) across all 360 OCT B scans per volume. The segmentation data from the OCT B scans were then applied to the phase-variance OCT-A data to generate *en-face* images of the OCTA volume between the OPL and RPE layers to isolate the CNV from retinal vessels. The size of the CNV was quantified by manually tracing the neovascular lesion on these en-face OCT-A images using FIJI image processing software.[45]

Flatmount immunohistochemistry

Eye cups were fixed with 4% paraformaldehyde (PFA) for 1 h and washed with PBS. The retinae were carefully removed, and the remaining RPE-choroid and scleral tissues were radially cut and labelled with Alexa Fluor 488-conjugated isolectin B4 (Invitrogen, I21411) overnight at 4°C. Fluorescence images were captured with confocal microscopy (Olympus FV1000), and CNV sizes were measured by manually tracing the isolectin B4-stained lesions using FIJI software.[45]

GUIDE-seq off-target assessment

Genome-wide unbiased off-target assessment was performed using GUIDE-seq based on a previously published protocol.[20] One million HEK293T cells were electroporated with SpCas9 and gRNA vectors and a 500 pmol dsODN template using the Gene Pulser Xcell Electroporation System (BioRad, Hercules, CA, USA, 1652660). Cells were collected 48 h after electroporation, and genomic DNA was extracted for library preparation according to published methods.[20] MiSeq and

bioinformatics analyses were conducted at the DNA Technology Core Facilities at UC Davis Genome Center.

Sequence data were analyzed using the open-source *guideseq* software suite (v.1.02, https://github.com/tsailabSJ/guideseq).[51] The analysis steps included (1) demultiplexing pooled samples based on sample-specific dual-indexed barcodes; (2) consolidation of PCR duplicates whereby reads sharing the same unique molecular identifier (UMI) and the first 6 bases of genomic sequence are collapsed into a consensus to improve quantification of aligned read counts; (3) alignment of the demultiplexed consolidate reads to the reference genome (GRCh38) utilizing BWA-MEM (v.0.7.17-r1188)[52] with default parameters; (4) tabulation of aligned reads with respect to mapping positions on a genome-wide basis whereby the start of genome mapping positions are consolidated using a 10 bp sliding window, with windows having reads mapping to both + and - strands or to the same strand but amplified with both forward and reverse tag-specific primers, flagged as sites of potential DSBs with 25 bp of flanking reference sequence retrieved on either side of the most frequent start-mapping position in each flagged window using BEDTools (v.2.20.1–22-g9b17893)[53] and locally aligned to the intended target sequence using Smith-Waterman alignment; (5) off-target cleavage sites with >6 mismatches to the intended target and/or >2 mismatches to the protospacer-adjacent motif (PAM) sequence or sites that are present in the control sample were removed; and (6) identification of valid target and off-target sites passing the above filters with read counts expected to scale approximately linearly with cleavage rates. The default PAM used was NGG, with the analysis also repeated using the less-frequent NAG PAM.[54] No off-target sites were identified with the latter PAM.

SUPPLEMENTAL INFORMATION

Supplemental information can be found online at https://doi.org/10.1016/j.omtn.2022.04.015.

ACKNOWLEDGMENTS

The authors thank John Douglas McPherson at UC Davis Health Integrated Genetics and Genomics core facility and The Genomics Shared Resource, supported by the UC Davis Comprehensive Support Grant (CCSG) funded by NCI P30CA093373, for GUIDE-seq analyses and advice. G.Y. is supported by NIH R01 EY032238 and R21 EY031108, the BrightFocus Foundation, and the Macula Society. R.Z. is supported by NIH R01 EY026556 and R01 EY031098. Histological studies were conducted at the UC Davis Center for Vision Sciences Structure-Function core facility, AAV production was conducted at the Molecular Packaging and Construct core facility, and *in vivo* mouse imaging was conducted at the Small Animal Ocular Imaging core facility, all of which are supported by NIH P30 EY012576. The funding organizations did not play any role in the design or conduct of this retrospective study; the collection, management, analysis, or interpretation of data; or the preparation, review, approval, or submission decision of the manuscript. The content is solely the responsibility of the authors and does not necessarily represent the official views of the funding agencies.

AUTHOR CONTRIBUTIONS

G.Y. conceived of the study, and S.H.C. and G.Y. designed the experiments and analyzed data. S.H.C. performed the subretinal injections, laser-induced CNV, and sequencing studies. T.-N.S. performed PCR, *in vitro* transfection, and figure preparation. S.H.C. and T.N. performed ELISA. B.D. performed OCT and OCT-A, and R.M. and R.Z. advised on *in vivo* data analysis. B.D., T.L., and D.L.-S. assisted with laser-induced CNV and subretinal injections. G.Y. and S.H.C. wrote and critically edited the manuscript.

DECLARATION OF INTERESTS

G.Y. received research support from Clearside Biomedical, Genentech, and Iridex and personal fees for consultancy from Abbvie, Adverum, Alimera, Anlong, Bausch & Lomb, Clearside Biomedical, Endogena, Genentech, Gyroscope Therapeutics, Intergalactic Therapeutics, Iridex, NGM Biopharmaceutical, Regeneron, Thea, Topcon, and Zeiss, all of which are unrelated to the contents of this study. The other authors have no relevant conflicts of interest.

REFERENCES

1. Todorich, B., Yiu, G., and Hahn, P. (2014). Current and investigational pharmacotherapeutic approaches for modulating retinal angiogenesis. Expert Rev. Clin. Pharmacol. *7*, 375–391. https://doi.org/10.1586/17512433.2014.890047.

2. Paulus, Y.M., and Sodhi, A. (2017). Anti-angiogenic therapy for retinal disease. Handb. Exp. Pharmacol. *242*, 271–307. https://doi.org/10.1007/164_2016_78.

3. Miller, J.W., Le Couter, J., Strauss, E.C., and Ferrara, N. (2013). Vascular endothelial growth factor a in intraocular vascular disease. Ophthalmology *120*, 106–114. https://doi.org/10.1016/j.ophtha.2012.07.038.

4. Bhutto, I.A., McLeod, D.S., Hasegawa, T., Kim, S.Y., Merges, C., Tong, P., and Lutty, G.A. (2006). Pigment epithelium-derived factor (PEDF) and vascular endothelial growth factor (VEGF) in aged human choroid and eyes with age-related macular degeneration. Exp. Eye Res. *82*, 99–110. https://doi.org/10.1016/j.exer.2005.05.007.

5. Solomon, S.D., Lindsley, K.B., Krzystolik, M.G., Vedula, S.S., and Hawkins, B.S. (2016). Intravitreal bevacizumab versus ranibizumab for treatment of neovascular age-related macular degeneration: findings from a cochrane systematic review. Ophthalmology *123*, 70–77. https://doi.org/10.1016/j.ophtha.2015.09.002.

6. Sarwar, S., Clearfield, E., Soliman, M.K., Sadiq, M.A., Baldwin, A.J., Hanout, M., Agarwal, A., Sepah, Y.J., Do, D.V., and Nguyen, Q.D. (2016). Aflibercept for neovascular age-related macular degeneration. Cochrane Database Syst. Rev. *2016*, CD011346. https://doi.org/10.1002/14651858.cd011346.pub2.

7. Campochiaro, P.A., Lauer, A.K., Sohn, E.H., Mir, T.A., Naylor, S., Anderton, M.C., Kelleher, M., Harrop, R., Ellis, S., and Mitrophanous, K.A. (2017). Lentiviral vector gene transfer of endostatin/angiostatin for macular degeneration (GEM) study. Hum. Gene Ther. *28*, 99–111. https://doi.org/10.1089/hum.2016.117.

8. Constable, I.J., Pierce, C.M., Lai, C.M., Magno, A.L., Degli-Esposti, M.A., French, M.A., McAllister, I.L., Butler, S., Barone, S.B., Schwartz, S.D., et al. (2016). Phase 2a randomized clinical trial: safety and post hoc analysis of subretinal rAAV.sFLT-1 for wet age-related macular degeneration. EBioMedicine *14*, 168–175. https://doi.org/10.1016/j.ebiom.2016.11.016.

9. Rakoczy, E.P., Lai, C.M., Magno, A.L., Wikstrom, M.E., French, M.A., Pierce, C.M., Schwartz, S.D., Blumenkranz, M.S., Chalberg, T.W., Degli-Esposti, M.A., and Constable, I.J. (2015). Gene therapy with recombinant adeno-associated vectors for neovascular age-related macular degeneration: 1 year follow-up of a phase 1 randomised clinical trial. Lancet *386*, 2395–2403. https://doi.org/10.1016/s0140-6736(15)00345-1.

10. Yiu, G. (2018). Genome editing in retinal diseases using CRISPR technology. Ophthalmol. Retina *2*, 1–3. https://doi.org/10.1016/j.oret.2017.09.015.

11. Yiu, G., Tieu, E., Nguyen, A.T., Wong, B., and Smit-McBride, Z. (2016). Genomic disruption of VEGF-A expression in human retinal pigment epithelial cells using

CRISPR-cas9 endonuclease. Invest. Ophthalmol. Vis. Sci. *57*, 5490–5497. https://doi.org/10.1167/iovs.16-20296.

12. Chung, S.H., Mollhoff, I.N., Nguyen, U., Nguyen, A., Stucka, N., Tieu, E., Manna, S., Meleppat, R.K., Zhang, P., Nguyen, E.L., et al. (2020). Factors impacting efficacy of AAV-mediated CRISPR-based genome editing for treatment of choroidal neovascularization. Mol. Ther. Methods Clin. Dev. *17*, 409–417. https://doi.org/10.1016/j.omtm.2020.01.006.

13. Huang, X., Zhou, G., Wu, W., Duan, Y., Ma, G., Song, J., Xiao, R., Vandenberghe, L., Zhang, F., D'Amore, P.A., and Lei, H. (2017). Genome editing abrogates angiogenesis in vivo. Nat. Commun. *8*, 112. https://doi.org/10.1038/s41467-017-00140-3.

14. Kim, E., Koo, T., Park, S.W., Kim, D., Kim, K., Cho, H.Y., Song, D.W., Lee, K.J., Jung, M.H., Kim, S., et al. (2017). In vivo genome editing with a small Cas9 orthologue derived from Campylobacter jejuni. Nat. Commun. *8*, 14500. https://doi.org/10.1038/ncomms14500.

15. Holmgaard, A., Askou, A.L., Benckendorff, J.N.E., Thomsen, E.A., Cai, Y., Bek, T., Mikkelsen, J.G., and Corydon, T.J. (2017). In vivo knockout of the Vegfa gene by lentiviral delivery of CRISPR/Cas9 in mouse retinal pigment epithelium cells. Mol. Ther. Nucleic Acids *9*, 89–99. https://doi.org/10.1016/j.omtn.2017.08.016.

16. Ling, S., Yang, S., Hu, X., Yin, D., Dai, Y., Qian, X., Wang, D., Pan, X., Hong, J., Sun, X., et al. (2021). Lentiviral delivery of co-packaged Cas9 mRNA and a Vegfa-targeting guide RNA prevents wet age-related macular degeneration in mice. Nat. Biomed. Eng. *5*, 144–156. https://doi.org/10.1038/s41551-020-00656-y.

17. Tsai, Y.T., Wu, W.H., Lee, T.T., Wu, W.P., Xu, C.L., Park, K.S., Cui, X., Justus, S., Lin, C.S., Jauregui, R., et al. (2018). Clustered regularly interspaced short palindromic repeats-based genome surgery for the treatment of autosomal dominant retinitis pigmentosa. Ophthalmology *125*, 1421–1430. https://doi.org/10.1016/j.ophtha.2018.04.001.

18. Maeder, M.L., Stefanidakis, M., Wilson, C.J., Baral, R., Barrera, L.A., Bounoutas, G.S., Bumcrot, D., Chao, H., Ciulla, D.M., DaSilva, J.A., et al. (2019). Development of a gene-editing approach to restore vision loss in Leber congenital amaurosis type 10. Nat. Med. *25*, 229–233. https://doi.org/10.1038/s41591-018-0327-9.

19. Keyt, B.A., Berleau, L.T., Nguyen, H.V., Chen, H., Heinsohn, H., Vandlen, R., and Ferrara, N. (1996). The carboxyl-terminal domain (111-165) of vascular endothelial growth factor is critical for its mitogenic potency. J. Biol. Chem. *271*, 7788–7795. https://doi.org/10.1074/jbc.271.13.7788.

20. Tsai, S.Q., Zheng, Z., Nguyen, N.T., Liebers, M., Topkar, V.V., Thapar, V., Wyvekens, N., Khayter, C., Iafrate, A.J., Le, L.P., et al. (2015). GUIDE-seq enables genome-wide profiling of off-target cleavage by CRISPR-Cas nucleases. Nat. Biotechnol. *33*, 187–197. https://doi.org/10.1038/nbt.3117.

21. Kim, K., Park, S.W., Kim, J.H., Lee, S.H., Kim, D., Koo, T., Kim, K.E., Kim, J.H., and Kim, J.S. (2017). Genome surgery using Cas9 ribonucleoproteins for the treatment of age-related macular degeneration. Genome Res. *27*, 419–426. https://doi.org/10.1101/gr.219089.116.

22. Huang, X., Zhou, G., Wu, W., Ma, G., D'Amore, P.A., Mukai, S., and Lei, H. (2017). Editing VEGFR2 blocks VEGF-induced activation of akt and tube formation. Invest. Ophthalmol. Vis. Sci. *58*, 1228–1236. https://doi.org/10.1167/iovs.16-20537.

23. Yamazaki, Y., and Morita, T. (2006). Molecular and functional diversity of vascular endothelial growth factors. Mol. Divers. *10*, 515–527. https://doi.org/10.1007/s11030-006-9027-3.

24. Rosen, L.S. (2002). Clinical experience with angiogenesis signaling inhibitors: focus on vascular endothelial growth factor (VEGF) blockers. Cancer Control *9*, 36–44. https://doi.org/10.1177/107327480200902s05.

25. Takahashi, K., Igarashi, T., Miyake, K., Kobayashi, M., Yaguchi, C., Iijima, O., Yamazaki, Y., Katakai, Y., Miyake, N., Kameya, S., et al. (2017). Improved intravitreal AAV-mediated inner retinal gene transduction after surgical internal limiting membrane peeling in cynomolgus monkeys. Mol. Ther. *25*, 296–302. https://doi.org/10.1016/j.ymthe.2016.10.008.

26. Carlevaro, M.F., Cermelli, S., Cancedda, R., and Descalzi Cancedda, F. (2000). Vascular endothelial growth factor (VEGF) in cartilage neovascularization and chondrocyte differentiation: auto-paracrine role during endochondral bone formation. J. Cell Sci. *113*, 59–69. https://doi.org/10.1242/jcs.113.1.59.

27. Saishin, Y., Saishin, Y., Takahashi, K., Silva, R.L.e., Hylton, D., Rudge, J.S., Wiegand, S.J., and Campochiaro, P.A. (2003). VEGF-TRAP(R1R2) suppresses choroidal neovascularization and VEGF-induced breakdown of the blood-retinal barrier. J. Cell Physiol. *195*, 241–248. https://doi.org/10.1002/jcp.10246.

28. Shah, C.P., Garg, S.J., Vander, J.F., Brown, G.C., Kaiser, R.S., and Haller, J.A.; Post-Injection Endophthalmitis (PIE) Study Team (2011). Outcomes and risk factors associated with endophthalmitis after intravitreal injection of anti-vascular endothelial growth factor agents. Ophthalmology *118*, 2028–2034. https://doi.org/10.1016/j.ophtha.2011.02.034.

29. Penn, J.S., Madan, A., Caldwell, R.B., Bartoli, M., Caldwell, R.W., and Hartnett, M.E. (2008). Vascular endothelial growth factor in eye disease. Prog. Retin. Eye Res. *27*, 331–371. https://doi.org/10.1016/j.preteyeres.2008.05.001.

30. Marneros, A.G., Fan, J., Yokoyama, Y., Gerber, H.P., Ferrara, N., Crouch, R.K., and Olsen, B.R. (2005). Vascular endothelial growth factor expression in the retinal pigment epithelium is essential for choriocapillaris development and visual function. Am. J. Pathol. *167*, 1451–1459. https://doi.org/10.1016/s0002-9440(10)61231-x.

31. Nishida, Y., Yamada, Y., Kanemaru, H., Ohazama, A., Maeda, T., and Seo, K. (2018). Vascularization via activation of VEGF-VEGFR signaling is essential for peripheral nerve regeneration. Biomed. Res. *39*, 287–294. https://doi.org/10.2220/biomedres.39.287.

32. Wang, H., Smith, G.W., Yang, Z., Jiang, Y., McCloskey, M., Greenberg, K., Geisen, P., Culp, W.D., Flannery, J., Kafri, T., et al. (2013). Short hairpin RNA-mediated knockdown of VEGFA in Muller cells reduces intravitreal neovascularization in a rat model of retinopathy of prematurity. Am. J. Pathol. *183*, 964–974. https://doi.org/10.1016/j.ajpath.2013.05.011.

33. Kurihara, T., Westenskow, P.D., Bravo, S., Aguilar, E., and Friedlander, M. (2012). Targeted deletion of Vegfa in adult mice induces vision loss. J. Clin. Invest. *122*, 4213–4217. https://doi.org/10.1172/jci65157.

34. Grunwald, J.E., Pistilli, M., Ying, G.S., Maguire, M.G., Daniel, E., and Martin, D.F.; Comparison of Age-related Macular Degeneration Treatments Trials Research Group (2015). Growth of geographic atrophy in the comparison of age-related macular degeneration treatments trials. Ophthalmology *122*, 809–816. https://doi.org/10.1016/j.ophtha.2014.11.007.

35. Grunwald, J.E., Daniel, E., Huang, J., Ying, G.S., Maguire, M.G., Toth, C.A., Jaffe, G.J., Fine, S.L., Blodi, B., Klein, M.L., et al. (2014). Risk of geographic atrophy in the comparison of age-related macular degeneration treatments trials. Ophthalmology *121*, 150–161. https://doi.org/10.1016/j.ophtha.2013.08.015.

36. Jo, D.H., Koo, T., Cho, C.S., Kim, J.H., Kim, J.S., and Kim, J.H. (2019). Long-term effects of in vivo genome editing in the mouse retina using Campylobacter jejuni Cas9 expressed via adeno-associated virus. Mol. Ther. *27*, 130–136. https://doi.org/10.1016/j.ymthe.2018.10.009.

37. Frock, R.L., Hu, J., Meyers, R.M., Ho, Y.J., Kii, E., and Alt, F.W. (2015). Genome-wide detection of DNA double-stranded breaks induced by engineered nucleases. Nat. Biotechnol. *33*, 179–186. https://doi.org/10.1038/nbt.3101.

38. Hu, J., Meyers, R.M., Dong, J., Panchakshari, R.A., Alt, F.W., and Frock, R.L. (2016). Detecting DNA double-stranded breaks in mammalian genomes by linear amplification-mediated high-throughput genome-wide translocation sequencing. Nat. Protoc. *11*, 853–871. https://doi.org/10.1038/nprot.2016.043.

39. Giannoukos, G., Ciulla, D.M., Marco, E., Abdulkerim, H.S., Barrera, L.A., Bothmer, A., Dhanapal, V., Gloskowski, S.W., Jayaram, H., Maeder, M.L., et al. (2018). UDiTaS, a genome editing detection method for indels and genome rearrangements. BMC Genomics *19*, 212. https://doi.org/10.1186/s12864-018-4561-9.

40. Ghezraoui, H., Piganeau, M., Renouf, B., Renaud, J.B., Sallmyr, A., Ruis, B., Oh, S., Tomkinson, A.E., Hendrickson, E.A., Giovannangeli, C., et al. (2014). Chromosomal translocations in human cells are generated by canonical nonhomologous end-joining. Mol. Cell *55*, 829–842. https://doi.org/10.1016/j.molcel.2014.08.002.

41. Nelson, C.E., Wu, Y., Gemberling, M.P., Oliver, M.L., Waller, M.A., Bohning, J.D., Robinson-Hamm, J.N., Bulaklak, K., Castellanos Rivera, R.M., Collier, J.H., et al. (2019). Long-term evaluation of AAV-CRISPR genome editing for Duchenne muscular dystrophy. Nat. Med. *25*, 427–432. https://doi.org/10.1038/s41591-019-0344-3.

42. Li, Y., Bolinger, J., Yu, Y., Glass, Z., Shi, N., Yang, L., Wang, M., and Xu, Q. (2019). Intracellular delivery and biodistribution study of CRISPR/Cas9 ribonucleoprotein

loaded bioreducible lipidoid nanoparticles. Biomater. Sci. *7*, 596–606. https://doi.org/10.1039/c8bm00637g.

43. Chen, G., Abdeen, A.A., Wang, Y., Shahi, P.K., Robertson, S., Xie, R., Suzuki, M., Pattnaik, B.R., Saha, K., and Gong, S. (2019). A biodegradable nanocapsule delivers a Cas9 ribonucleoprotein complex for in vivo genome editing. Nat. Nanotechnol. *14*, 974–980. https://doi.org/10.1038/s41565-019-0539-2.

44. Lyu, P., Javidi-Parsijani, P., Atala, A., and Lu, B. (2019). Delivering Cas9/sgRNA ribonucleoprotein (RNP) by lentiviral capsid-based bionanoparticles for efficient 'hit-and-run' genome editing. Nucleic Acids Res. *47*, e99. https://doi.org/10.1093/nar/gkz605.

45. Nihongaki, Y., Kawano, F., Nakajima, T., and Sato, M. (2015). Photoactivatable CRISPR-Cas9 for optogenetic genome editing. Nat. Biotechnol. *33*, 755–760. https://doi.org/10.1038/nbt.3245.

46. Chen, X., Chen, Y., Xin, H., Wan, T., and Ping, Y. (2020). Near-infrared optogenetic engineering of photothermal nanoCRISPR for programmable genome editing. Proc. Natl. Acad. Sci. U S A *117*, 2395–2405. https://doi.org/10.1073/pnas.1912220117.

47. Li, F., Hung, S.S.C., Mohd Khalid, M.K.N., Wang, J.H., Chrysostomou, V., Wong, V.H.Y., Singh, V., Wing, K., Tu, L., Bender, J.A., et al. (2019). Utility of self-destructing CRISPR/Cas constructs for targeted gene editing in the retina. Hum. Gene Ther. *30*, 1349–1360. https://doi.org/10.1089/hum.2019.021.

48. Chung, S.H., Mollhoff, I.N., Mishra, A., Sin, T.N., Ngo, T., Ciulla, T., Sieving, P., Thomasy, S.M., and Yiu, G. (2021). Host immune responses after suprachoroidal delivery of AAV8 in nonhuman primate eyes. Hum. Gene Ther. *32*, 682–693. https://doi.org/10.1089/hum.2020.281.

49. Fernandez-Godino, R., Garland, D.L., and Pierce, E.A. (2016). Isolation, culture and characterization of primary mouse RPE cells. Nat. Protoc. *11*, 1206–1218. https://doi.org/10.1038/nprot.2016.065.

50. Zhang, P., Zam, A., Jian, Y., Wang, X., Li, Y., Lam, K.S., Burns, M.E., Sarunic, M.V., Pugh, E.N., Jr., and Zawadzki, R.J. (2015). In vivo wide-field multispectral scanning laser ophthalmoscopy-optical coherence tomography mouse retinal imager: longitudinal imaging of ganglion cells, microglia, and Muller glia, and mapping of the mouse retinal and choroidal vasculature. J. Biomed. Opt. *20*, 126005. https://doi.org/10.1117/1.jbo.20.12.126005.

51. Tsai, S.Q., Topkar, V.V., Joung, J.K., and Aryee, M.J. (2016). Open-source guideseq software for analysis of GUIDE-seq data. Nat. Biotechnol. *34*, 483. https://doi.org/10.1038/nbt.3534.

52. Li, H. (2013). Aligning sequence reads, clone sequences and assembly contigs with BWA-MEM. Preprint at arXiv. https://doi.org/10.48550/arXiv.1303.3997.

53. Quinlan, A.R., and Hall, I.M. (2010). BEDTools: a flexible suite of utilities for comparing genomic features. Bioinformatics *26*, 841–842. https://doi.org/10.1093/bioinformatics/btq033.

54. Hsu, P.D., Scott, D.A., Weinstein, J.A., Ran, F.A., Konermann, S., Agarwala, V., Li, Y., Fine, E.J., Wu, X., Shalem, O., et al. (2013). DNA targeting specificity of RNA-guided Cas9 nucleases. Nat. Biotechnol. *31*, 827–832. https://doi.org/10.1038/nbt.2647.